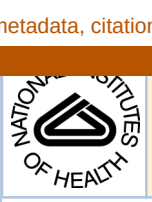

Published in final edited form as:

J Struct Biol. 2011 January ; 173(1): 146–152. doi:10.1016/j.jsb.2010.08.003.

Nanoscale Morphology of Type I Collagen is Altered in the Brtl Mouse Model of Osteogenesis Imperfecta

Joseph M. Wallace[a,b], **Bradford G. Orr**[b,c,d], **Joan C. Marini**[g], and **Mark M. Banaszak Holl**[a,b,d,e,f]

Joseph M. Wallace: jmwallac@umich.edu; Bradford G. Orr: orr@umich.edu; Joan C. Marini: oidoc@helix.nih.gov; Mark M. Banaszak Holl: mbanasza@umich.edu

[a] University of Michigan, Department of Chemistry

[b] University of Michigan, Michigan Nanotechnology Institute for Medicine and Biological Science

[c] University of Michigan, Department of Physics

[d] University of Michigan, Program in Applied Physics

[e] University of Michigan, Program in Biophysics

[f] University of Michigan, Program Macromolecular Science and Engineering

[g] Bone and Extracellular Matrix Branch, The Eunice Kennedy Shriver National Institute of Child Health and Human Development (NICHD), NIH

Abstract

Bone has a complex hierarchical structure that has evolved to serve structural and metabolic roles in the body. Due to the complexity of bone structure and the number of diseases which affect the ultrastructural constituents of bone, it is important to develop quantitative methods to assess bone nanoscale properties. Autosomal dominant Osteogenesis Imperfecta results predominantly from glycine substitutions (80%) and splice site mutations (20%) in the genes encoding the α1 or α2 chains of Type I collagen. Genotype-phenotype correlations using over 830 collagen mutations have revealed that lethal mutations are located in regions crucial for collagen-ligand binding in the matrix. However, few of these correlations have been extended to collagen structure in bone. Here, an atomic force microscopy-based approach was used to image and quantitatively analyze the D-periodic spacing of Type I collagen fibrils in femora from heterozygous (Brtl/+) mice (α1(I)G349C), compared to wild type (WT) littermates. This disease system has a well-defined change in the *col1α1* allele, leading to a well characterized alteration in collagen protein structure, which are directly related to altered Type I collagen nanoscale morphology, as measured by the D-periodic spacing. In Brtl/+ bone, the D-periodic spacing shows significantly greater variability on

Corresponding Authors: Dr. Joseph M. Wallace, University of Michigan, Department of Chemistry, 930 N. University Ave., Ann Arbor, MI 48109-1055, Ph: (734) 678-0245, Fax: (734) 615-2506, jmwallac@umich.edu. Dr. Mark M. Banaszak Holl, University of Michigan, Department of Chemistry, 930 N. University Ave., Ann Arbor, MI 48109-1055, Ph: (734) 763-2283, Fax: (734) 763-2283, mbanasza@umich.edu.

Authors' Contributions

Joseph M Wallace: Experimental design, data collection, data analysis

Bradford G. Orr: Data analysis

Joan C. Marini: OI expertise and experimental design; Provided sacrificed Brtl and WT mice under MTA with U of Michigan

Mark M. Banaszak Holl: Experimental design, data analysis

average and along the length of the bone compared to WT, although the average spacing was unchanged. Brtl/+ bone also had a significant difference in the population distribution of collagen D-period spacings. These changes may be due to the mutant collagen structure, or to the heterogeneity of collagen monomers in the Brtl/+ matrix. These observations at the nanoscale level provide insight into the structural basis for changes present in bone composition, geometry and mechanical integrity in Brtl/+ bones. Further studies are necessary to link these morphological observations to nanoscale mechanical integrity.

Keywords

AFM; Ultrastructure; Nanoscale; 2D FFT; Genotype/Phenotype

Introduction

Bone is an elegant biomaterial with a complex hierarchical organization that has evolved to serve a number of structural and metabolic functions. Bone is a two-phase composite composed of a ductile organic matrix (~90% Type I collagen) which is reinforced by a carbonated apatite mineral phase. Many would argue that the mechanical properties of these constituent components of bone largely control the mechanical properties of the bone itself.[1] Despite the importance of skeletal health to overall health, it is still not clear how the nanoscale properties of collagen and mineral in bone, and their intimate interaction with one another, translate into the mechanical integrity of the structure that develops at higher levels of the bone hierarchy. [2,3] Further, it is not fully understood how alterations to the individual constituents can change the mechanical competence of the bone. One recent study elegantly illustrated how changes to even ancillary components of the bone matrix can drastically alter properties across the bone hierarchy. [4] It is therefore important for researchers to develop new quantitative methods to assess the nanoscale properties of normal bone and to study how these properties change in response to disease.[5]

Type I collagen forms the template upon which all bones are built. Collagen is initially synthesized as a polypeptide chain of amino acids (Figure 1) with an uninterrupted region of repeating Gly-X-Y triplets (X and Y are often proline and hydroxyproline, respectively).[6] Glycine has the smallest amino acid side chain (a single hydrogen atom). The significance of glycine being present as every third amino acid is that this small side chain can be accommodated within the central axis of a left-handed helical structure (the α helix). Other amino acids with larger, bulkier side chains would prevent proper folding of the helix. Three of these helical chains come together to form a right-handed triple helix. Once secreted from the cell, non-helical propeptide ends are enzymatically cleaved, leaving a tropocollagen molecule. Tropcollagen molecules self-assemble in a staggered, parallel manner to form a 3D fibril. Because of the space between the ends of the tropocollagen molecules and the offset from row to row, regions of gaps and overlaps exist within the fibril and produce an oscillating surface topography with a characteristic axial repeat pattern called the D-periodicity.

Type I collagen is a heterotrimeric molecule composed of two α1 chains and one α2 chain. Mutations in the genes encoding the α chains can cause diseases of bone and other tissues such as Osteogenesis Imperfecta (OI), or brittle bone disease, and some forms of Ehlers-Danlos Syndrome. Human OI results primarily from point mutations that cause the substitution of a glycine residue in the triple helical region (80%) or splice site mutations (20%) in the genes encoding the α1 or α2 chains of Type I collagen. [7,8] The disease displays a wide spectrum of clinical severities, with more severe forms arising from changes in the primary amino acid sequence. These changes in alpha chain structure result in delayed

protein folding and over-modification of the collagen triple helix, and decrease collagen quality [9], although disease severity does not correlate with the extent of collagen over-modification. Milder forms of dominant OI arise from null mutations in one Type I collagen allele, resulting in an underproduction of normal collagen. Depending on the severity of the disease, symptoms range from susceptibility to fracture from mild trauma to perinatal lethality.

Correlations between genotype and phenotype in OI utilizing over 800 mutations revealed that mutations in the Major Ligand Binding Regions in the α1 chain and the proteoglycan binding regions in the α2 chain were almost entirely lethal. [8] Histomorphometry of OI bone has shown that surface-based remodelling parameters are increased in all forms of OI but that mineralization defects are not present [10] (with the possible exception of Type VI OI [9]). Some studies have investigated the impact of OI mutations on the structure and mechanical integrity of non-mineralized tendon [11,12] or on the properties of the mineral in OI bone [13], but correlations between genotype and collagen structure in OI bone are limited. [14,15] The Brittle (Brtl) mouse, a model of human Type IV OI which has a classical glycine substitution (a cysteine is substituted for a glycine at the 349 position of the triple helix, Figure 1) in one *col1α1* allele, was created to study how specific changes in the amino acid sequence of collagen can lead to OI phenotypic characteristics.[16]

The need for quantitative analytical methods to assess the nanoscale morphology of collagen in bone without tissue disruption has prompted us to study the collagen ultrastructure of bone using atomic force microscopy (AFM). [17,18] In comparison to other high-resolution methods used to assess the nanoscale properties of bone and other mineralized tissues, [19,20] AFM is less destructive and requires less sample preparation, [21] implying that measured properties are less likely artifacts of sample processing or imaging. It was previously shown that normal Type I collagen-based tissues, including bone, contain a distribution of Type I collagen fibril morphologies, as measured by the fibril D-periodic spacing.[17,18] We further demonstrated that estrogen-depletion in sheep leads to a significant change in this distribution in bone.[17] However, because the effects of estrogen and estrogen depletion on collagen structure are not well understood, it was not possible to ascribe a mechanism to these changes in collagen morphology. The current study was undertaken in an attempt to study ultrastructural changes in collagen fibril structure following a defined genetic insult. AFM was used to image and quantitatively analyze the D-periodic spacing of Type I collagen fibrils in intact and mineralized bones from wild type (WT) and heterozygous (Brtl/+) mice. This disease system has a well-defined change in the *col1α1* allele and in collagen protein structure. It was hypothesized that changes in the mean D-periodic spacing as well as alterations in the D-period population distribution, might also be present in diseased fibrils from Brtl/+ mice in comparison to their WT littermates. Although the average D-periodic spacing was not significantly different in Brtl/+ versus WT bone, the D-periodic spacing in Brtl/+ bone had greater variability overall and along the length of the bone. A significant difference in the population distributions of collagen D-periodic spacing was also present in Brtl/+ bone. These nanoscale observations provide insight into the structural basis for changes present in bone composition, geometry and mechanical integrity in Brtl/+ bones.

Materials and Methods

Animals

Brtl/+ and WT mice from the mixed Sv129/CD-1/C57BL/6S background strain were used with prior approval of the NICHD Animal Care Committee (protocol # ASP 09-023) and were sacrificed by lethal injection. Femurs from two month-old male wild type (WT, n=4)

and Brtl/+ (n=4) mice were harvested and stripped of soft tissue before processing for imaging.

Atomic Force Microscopy (AFM) imaging and analysis

Before use, the proximal (above the third trochanter) and distal ends of each right femur were removed using a low-speed sectioning saw (Figure 2). The marrow cavity of each bone was cleaned using a small tube brush. Bones were mounted, anterior-side up, to a steel disk using a thin layer of cyanoacrylate glue. A flat polished surface of intracortical bone was created using a 3 μm polycrystalline water-based diamond suspension and a 0.05 μm deagglomerated alumina suspension (Buehler LTD; Lake Bluff, Il). The bones were sonicated for 15 seconds to remove polishing residue and debris. To remove extrafibrillar surface mineral and expose underlying collagen fibrils, the surface of each bone was demineralized using 0.5M EDTA at a pH of 8.0 for 15 minutes, then vigorously rinsed with ultrapure water and soaked at 4°C for at least 16 hours. EDTA is often used in mineralized tissue research to remove mineral while keeping collagen and cells intact and viable. [22,23] Before imaging, each sample was briefly sonicated to remove any mineral that was still bound to the surface.

Samples were imaged in air using a PicoPlus 5500 AFM (Agilent). Images were acquired in tapping mode using silicon cantilevers (VistaProbes T300R, tip radius < 10 nm, force constant 40 N/m, resonance frequency 300 kHz; nanoScience Instruments; Phoenix, AZ) at line scan rates of 2 Hz or lower at 512 lines per frame.

Making absolute x-y distance measurements with AFM has multiple limitations. Prior to sampling, calibration of the system was performed according manufacturer guidelines. A calibration grating with a 10 μm period was imaged with the scan size set just under the range of the piezo (80 μm scan size) at 512 pixels by 512 pixels. This results in a pixel size of roughly 160 nm. To overcome limitations imposed by pixel size, multiple consecutive periods were measured. The measured period was defined as the total measured length divided by the number of periods. The calibration was adjusted until the measured period was within 25 nm of the actual 10 μm period. This calibration method results in a maximum error of 0.25%, which is less than the 1% tolerance specified by the manufacturer. For the imaging of collagen fibrils, scan sizes were reduced to 3.5 μm at 512 × 512 pixels. Because of the effective linearity of the piezo, error scales with the reduction of scan size, reducing the 25 nm tolerance to 1.1 nm.

Image Analysis

Images were acquired from 9 axial locations in each bone sample (designated 1–9 beginning at the proximal end of the sample, Figure 2). At each location, 70 μm × 70 μm scans were performed to find sites for closer inspection, then the scan size was decreased to a final size of 3.5 μm × 3.5 μm. Amplitude images were analyzed to investigate the D-periodic spacing, chosen as our key metric of fibril morphology (Figure 1). Five to ten fibrils from each axial location were analyzed (SPIP v5.0.6, Image Metrology; Hørsholm, Denmark). Following image capture, a rectangular region of interest (ROI) was chosen along straight segments of individual fibrils (Figure 3). The ROI was drawn to ensure that it started and ended at the edge of a gap zone, a method which minimizes edge effects that can degrade resolution. For each evaluated fibril, a two dimensional Fast Fourier Transform (2D FFT) was performed and the primary peak from the 2D power spectrum was analyzed to determine the value of the D-periodic spacing for that fibril. This process decouples the measured D-Period repeat distance from both pixel size and fibril orientation. A detailed analysis of the uncertainty associated with this type of measurement sets the minimum bin size for population studies at 0.8 nm. For all histograms, the bin size was therefore set at 1 nm.

Statistical Analysis

All statistical analyses utilized SPSS (Version 16.0, SPSS Inc.). For all investigations, a value of $p<0.05$ was considered significant. To investigate differences in fibril morphology as a function of genotype, D-periodic spacing values measured from an individual bone sample were averaged, yielding an single value for that sample. The values from WT (n=4) and Brtl/+ (n=4) mice were then compared using One Way ANOVA.

To examine differences in the distribution of fibril morphology between genotypes, histograms and the Cumulative Distribution Function (CDF) of each group were computed. The CDF shows the fraction of a given sample which is contained up to a particular value, easily demonstrating differences between distributions in both mean and standard deviation. To test for statistically significant differences between distributions, Kolmogorov-Smirnov (K-S) tests were applied to the data. This test is sensitive to changes in both the mean value and standard deviation of a distribution.

Results

The D-periodic spacing was chosen as the key metric of fibril morphology (Figure 1). This measure captures aspects of fibril structure which may be related to the state of the individual molecular triple helices, post-translational modifications and cross-linking. To quantitatively assess the D-periodic spacing in murine cortical bone as a function of OI genotype, femora from 2 month old male mice were used. In the intracortical bone along the anterior surface of the diaphysis, 9 locations were analyzed in each sample. Five to ten fibrils were analyzed at each axial location. Within each genotype, measurements at each axial location were pooled to assess the variability in morphology along the length of the femur (Figure 4). The spread of the data at each axial location is qualitatively larger in the Brtl/+ bones (B) in comparison to the WT (A) bones.

All measurements within each bone were averaged to yield the mean fibril spacing for that bone, then the 4 WT values were compared with the 4 Brtl/+ values (Figure 5). Within each genotype, the overall mean values were 67.6 nm and 67.4 nm for WT and Brtl/+, respectively. There was no significant effect of genotype on mean fibril spacing ($p=0.392$) when the mean values from the 4 bones in each genotype were compared by One Way ANOVA.

In addition to mean differences in morphology, important information can also be obtained by viewing the population distribution of fibril morphologies within each genotype (Figure 6). Figure 6A shows that a distribution of spacings exists in each genotype and that these distributions differ between WT and dysplastic bone. The main population of fibrils in each group was defined using the mean of the WT group ± 1 standard deviation, which is 66 - 70 nm (Figure 6A). Within this range, 75% of WT, but only 55% of Brtl/+ fibrils, were found. As a second method to visualize these distributions, the Cumulative Distribution Function (CDF) was computed from the measurements in each group (Figure 6B). Both the histogram and the CDF indicate that the Brtl/+ bones have populations of fibrils with both closer and longer spacings than does the WT group. To test for statistically significant differences between distributions, a fundamentally different comparison than the difference in means tested above using One Way ANOVA, Kolmogorov-Smirnov (K-S) tests were applied to the data. This test is sensitive to changes in both the mean value and standard deviation of a distribution. The population distribution of the D-periodic spacings in Brtl/+ bones was significantly different than the WT bones ($p=0.001$).

Discussion

In this study, surface characterization of Type I collagen at the nanoscale was linked with biology in an effort to understand the ultrastructural mechanisms of an Osteogenesis Imperfecta (OI) phenotype in bone. Normal bone contains a distribution of Type I collagen fibril morphologies, as measured by the fibril D-periodic spacing. [17,18] A previous study in sheep subjected to two years of ovariectomy-induced estrogen depletion demonstrated a quantifiable change in this distribution as a function of the disease state. [17] However, the direct effects of estrogen-depletion on collagen are unknown and it is therefore difficult to understand why this change in the distribution of fibril morphologies exists. A major strength of the current study is that a disease system with a well-defined genetic change in the *col1α1* allele [16] and well characterized alterations in collagen protein structure [24–26] was directly related to alterations in Type I collagen nanoscale morphology. By characterizing the mean fibril D-spacing and the distribution of fibril morphologies in the bone of normal mice and mice that were heterozygous for a specific *col1a1* point mutation (G349C), phenotypic changes in the collagen fibril ultrastructure were detected. Studies are currently underway to begin linking these differences in ultrastructural morphology to alterations in the nanoscale mechanical behaviour of Type I collagen.

Although the mean D-periodic spacing of Type I collagen fibrils in Brtl/+ bone was not significantly different than in WT, the distribution of spacing values was distinctive between the genotypes (Figure 6). Further, there was more variation in fibril morphology along the axial length of Brtl/+ bones (Figure 4). In light of what is known about the mutation in Brtl/+ mice [16] and its detrimental effects on collagen synthesis, [24,26,27] bone structure and overall bone mechanical integrity, [27] these findings at the nanoscale are important. Bones from Brtl/+ mice have normal levels of *col1a1* and *col1a2* transcripts, [25] and produce Type I collagen molecules with 3 different chain compositions (2 normal α1 chains, +/+; 1 normal and 1 mutant α1 chain, G349C/+; 2 mutant α1 chains, G349C/G349C) in an expected 1:2:1 ratio. Abnormal trafficking of collagen molecules with a single mutant chain leads to the accumulation of collagen in the endoplasmic reticulum resulting in delayed secretion, over modification and selective degradation [26]. As a result, among the total collagen molecules secreted from Brtl/+ cells, the proportion with a single mutant chain ranges from 26–40%, considerably lower than the theoretical 50%. [26] Once mutant molecules are secreted from cells, they are efficiently incorporated into collagen fibrils and form crosslinks with the same efficiency as in WT mice. [24,26]

Fibrils formed in Brtl/+ mice are thinner and exhibit a disruption of the normal quasi-crystalline lateral packing, but the methods used to measure these properties were indirect. [24] Data from the current study directly demonstrate that the incorporation of mutant molecules changes the intrafibrillar organization of collagen fibrils. Changes in the D-period spacing are likely driven by alterations in the end-to end spacing of collagen molecules within the fibril due to changes in intracellular tropocollagen processing and assembly, by a change in the tightness of the twist of the fibril, or even by differences in mineralization within the fibrils themselves. [28–30] Since collagen forms the template for mineralization, altered collagen may also account for changes in mineral composition and density [27,31] and may result in differences in the relationship between collagen and mineral. It is also possible that changes in the relationship between collagen, non-collagenous proteins and mineral are partially responsible for the observed changes in fibril morphology.

Recent modeling studies have investigated the effects of point mutations on collagen structure [32] and mechanical integrity. [33,34] Normal collagen helices and helices with single amino acid point mutations were modelled and the incorporation of these helices into triple helical tropocollagen molecules was investigated. The major conclusion from these

studies was that the alteration of the normal amino acid sequence leads to packing differences in collagen molecules which could contribute to the compromised mechanical integrity associated with OI. Specifically, at the single molecule level, OI mutations led to weakened intermolecular adhesion, increased intermolecular lateral spacing and, ultimately, decreased mechanical stiffness of individual tropocollagen molecules. Changes in these parameters scaled with the severity of the mutation. In addition, failure strength and yield strain were detrimentally impacted in collagen fibrils with the most severe mutations. A limitation of this fibrillar-level study is that a mesoscale model was used and the output of the nanomechanical investigation served only as an input parameter in the formulation of the model. Therefore, this model assumes that all tropocollagen molecules within the tested fibril are the same. As mentioned above, the heterozygous Brtl/+ model has three different chain compositions which are then randomly incorporated into fibrils, complicating the comparison to the current study. Here, changes in fibril D-periodicity caused by the alteration in amino acid sequence from a single point mutation in OI are directly observed, although this is a different measure of fibril spacing than the one mentioned in the modeling studies. Regardless, the theoretical results predict a wider range of intermolecular spacings, which may relate to the broader distribution of D-periodic spacing directly observed here.

In the current study, mutant bone had large percentages of fibrils with spacing that were either larger or smaller than the main population of the WT fibrils (defined as the mean ± 1 standard deviation). It is postulated that the large population of fibrils with spacings less than the mean minus 1 standard deviation of WT values observed here (~25% of all mutant fibrils) means that less space is available inside of these fibrils for water and mineral to occupy. The decrease in water will have a direct negative impact on the viscoelastic and post-yield behaviour of the fibril. Less space within these fibrils may also limit the ability of mineral to nucleate and grow within the confines of the fibrillar template.[15] If true, an increased proportion of extrafibrillar mineral could lead to the known hypermineralization phenotype that is characteristic of Brtl/+ mice.[27] Another possibility is that the population of fibrils with spacings greater that the main WT population (~15% of all mutant fibrils) have more space within the fibril which may allow mineral crystals to grow larger (also manifesting as increased mineralization) and become more brittle. The link between these alterations in fibril morphology and direct changes in the mechanical integrity of those fibrils requires further investigation.

Conclusion

In conclusion, the nanoscale morphology of Type I collagen, as measured by the fibril D-periodic spacing, was probed to gain a mechanistic understanding of changes induced in the collagen ultrastructure of bone in a murine model of Type IV Osteogenesis Imperfecta. Although the average D-periodic spacing in Brtl/+ bone was the same as WT, Brtl/+ bone shows greater variability of D-periodic spacing along the length of the bone and a significant difference in the population distribution of collagen fibrils. These observations at the nanoscale level provide insight into the structural basis for changes in bone composition, geometry and mechanical integrity in Brtl/+ bones. These changes in morphology may be directly related to alterations in nanoscale mechanical integrity, a hypothesis that requires additional study.

Acknowledgments

Acknowledgements and Funding Sources

This work was partially supported by the National Institute of Dental and Craniofacial Research (National Institutes of Health) through a Ruth L. Kirschstein National Service Award (Grant number 1F32DE018840-01 A1). JCM is

supported by NICHD Intramural Funding. The authors thank Wayne Cabral for generation of Brtl/WT mice used in these experiments.

References

1. Ritchie RO, Buehler MJ, Hansma P. Plasticity and toughness in bone. Phys Today 2009;62:41–47.
2. Gupta HS, Wagermaier W, Zickler GA, Raz-Ben Aroush D, Funari SS, Roschger P, Wagner HD, Fratzl P. Nanoscale deformation mechanisms in bone. Nano Lett 2005;5:2108–2111. [PubMed: 16218747]
3. Fratzl P, Gupta HS, Paschalis EP, Roschger P. Structure and mechanical quality of the collagen mineral nano-composite in bone. Journal of Materials Chemistry 2004;14:2115–2123.
4. Thurner PJ, Chen CG, Ionova-Martin S, Sun L, Harman A, Porter A, Ager JW III, Ritchie RO, Alliston T. Osteopontin deficiency increases bone fragility but preserves bone mass. Bone. 2010
5. Buehler MJ, Yung YC. Deformation and failure of protein materials in physiologically extreme conditions and disease. Nature Materials 2009;8:175–188.
6. Gerhard DS, Wagner L, Feingold EA, et al. The status, quality, and expansion of the NIH full-length cDNA project: the Mammalian Gene Collection (MGC). Genome Res 2004;14:2121–2127. [PubMed: 15489334]
7. Byers PH, Wallis GA, Willing MC. Osteogenesis imperfecta: translation of mutation to phenotype. J Med Genet 1991;28:433–442. [PubMed: 1895312]
8. Marini JC, Forlino A, Cabral WA, Barnes AM, San Antonio JD, Milgrom S, Hyland JC, Korkko J, Prockop DJ, De Paepe A. Consortium for osteogenesis imperfecta mutations in the helical domain of type I collagen: regions rich in lethal mutations align with collagen binding sites for integrins and proteoglycans. Hum Mutat 2007;28:209–221. [PubMed: 17078022]
9. Glorieux FH, Ward LM, Rauch F, Lalic L, Roughley PJ, Travers R. Osteogenesis imperfecta type VI: a form of brittle bone disease with a mineralization defect. J Bone Miner Res 2002;17:30–38. [PubMed: 11771667]
10. Rauch F, Travers R, Parfitt AM, Glorieux FH. Static and dynamic bone histomorphometry in children with osteogenesis imperfecta. Bone 2000;26:581–589. [PubMed: 10831929]
11. McBride DJ Jr, Choe V, Shapiro JR, Brodsky B. Altered collagen structure in mouse tail tendon lacking the alpha 2(I) chain. J Mol Biol 1997;270:275–284. [PubMed: 9236128]
12. Misof K, Landis WJ, Klaushofer K, Fratzl P. Collagen from the osteogenesis imperfecta mouse model (oim) shows reduced resistance against tensile stress. J Clin Invest 1997;100:40–45. [PubMed: 9202055]
13. Fratzl P, Paris O, Klaushofer K, Landis WJ. Bone mineralization in an osteogenesis imperfecta mouse model studied by small-angle x-ray scattering. J Clin Invest 1996;97:396–402. [PubMed: 8567960]
14. Cassella JP, Barber P, Catterall AC, Ali SY. A morphometric analysis of osteoid collagen fibril diameter in osteogenesis imperfecta. Bone 1994;15:329–334. [PubMed: 8068454]
15. Sarathchandra P, Pope FM, Ali SY. Morphometric analysis of type I collagen fibrils in the osteoid of osteogenesis imperfecta. Calcif Tissue Int 1999;65:390–395. [PubMed: 10541766]
16. Forlino A, Porter FD, Lee EJ, Westphal H, Marini JC. Use of the Cre/lox recombination system to develop a non-lethal knock-in murine model for osteogenesis imperfecta with an alpha1(I) G349C substitution. Variability in phenotype in BrtlIV mice. J Biol Chem 1999;274:37923–37931. [PubMed: 10608859]
17. Wallace JM, Erickson B, Les CM, Orr BG, Banaszak Holl MM. Distribution of Type I Collagen Morphologies in Bone: Relation to Estrogen Depletion. Bone 2010;46:1349–1354. [PubMed: 19932773]
18. Wallace JM, Chen Q, Fang M, Erickson B, Orr BG, Banaszak Holl MM. Type I Collagen Exists as a Distribution of Nanoscale Morphologies in Teeth, Bones and Tendons. Langmuir 2010;26:7349–7354. [PubMed: 20121266]
19. Giraud-Guille MM. Twisted plywood architecture of collagen fibrils in human compact bone osteons. Calcif Tissue Int 1988;42:167–180. [PubMed: 3130165]

20. Weiner S, Arad T, Sabanay I, Traub W. Rotated plywood structure of primary lamellar bone in the rat: orientations of the collagen fibril arrays. Bone 1997;20:509–514. [PubMed: 9177863]
21. Morris, VJ.; Kirby, AR.; Gunning, AP. Atomic force microscopy for biologists. Imperial College Press; Norwich, UK: 1999.
22. Jonsson R, Tarkowski A, Klareskog L. A demineralization procedure for immunohistopathological use. EDTA treatment preserves lymphoid cell surface antigens. J Immunol Methods 1986;88:109–114. [PubMed: 2420895]
23. Klein-Nulend J, Burger EH, Semeins CM, Raisz LG, Pilbeam CC. Pulsating fluid flow stimulates prostaglandin release and inducible prostaglandin G/H synthase mRNA expression in primary mouse bone cells. J Bone Miner Res 1997;12:45–51. [PubMed: 9240724]
24. Kuznetsova NV, Forlino A, Cabral WA, Marini JC, Leikin S. Structure, stability and interactions of type I collagen with GLY349-CYS substitution in alpha 1(I) chain in a murine Osteogenesis Imperfecta model. Matrix Biol 2004;23:101–112. [PubMed: 15246109]
25. Forlino A, Tani C, Rossi A, Lupi A, Campari E, Gualeni B, Bianchi L, Armini A, Cetta G, Bini L, Marini JC. Differential expression of both extracellular and intracellular proteins is involved in the lethal or nonlethal phenotypic variation of BrtlIV, a murine model for osteogenesis imperfecta. Proteomics 2007;7:1877–1891. [PubMed: 17520686]
26. Forlino A, Kuznetsova NV, Marini JC, Leikin S. Selective retention and degradation of molecules with a single mutant α1 (I) chain in the Brtl IV mouse model of OI. Matrix Biology 2007;26:604–614. [PubMed: 17662583]
27. Kozloff KM, Carden A, Bergwitz C, Forlino A, Uveges TE, Morris MD, Marini JC, Goldstein SA. Brittle IV mouse model for osteogenesis imperfecta IV demonstrates postpubertal adaptations to improve whole bone strength. J Bone Miner Res 2004;19:614–622. [PubMed: 15005849]
28. Israelowitz M, Rizvi SWH, Kramer J, von Schroeder HP. Computational modeling of type I collagen fibers to determine the extracellular matrix structure of connective tissues. Protein Engineering Design and Selection 2005;18:329–335.
29. Zhang W, Liao S, Cui F. Hierarchical self-assembly of nano-fibrils in mineralized collagen. Chem Mater 2003;15:3221–3226.
30. Beniash E, Traub W, Veis A, Weiner S. A transmission electron microscope study using vitrified ice sections of predentin: structural changes in the dentin collagenous matrix prior to mineralization. J Struct Biol 2000;132:212–225. [PubMed: 11243890]
31. Kozloff, KM. PhD Dissertation. University of Michigan; 2005. Influence of a Collagen Mutation on the Mechanical Nature of Bone: Governing Factors in a Disease Model For Osteogenesis Imperfecta Type IV.
32. Bella J, Eaton M, Brodsky B, Berman HM. Crystal and molecular structure of a collagen-like peptide at 1.9 A resolution. Science 1994;266:75. [PubMed: 7695699]
33. Gautieri A, Uzel S, Vesentini S, Redaelli A, Buehler MJ. Molecular and mesoscale mechanisms of osteogenesis imperfecta disease in collagen fibrils. Biophys J 2009;97:857–865. [PubMed: 19651044]
34. Gautieri A, Vesentini S, Redaelli A, Buehler MJ. Single molecule effects of osteogenesis imperfecta mutations in tropocollagen protein domains. Protein Science 2009;18:161–168. [PubMed: 19177360]

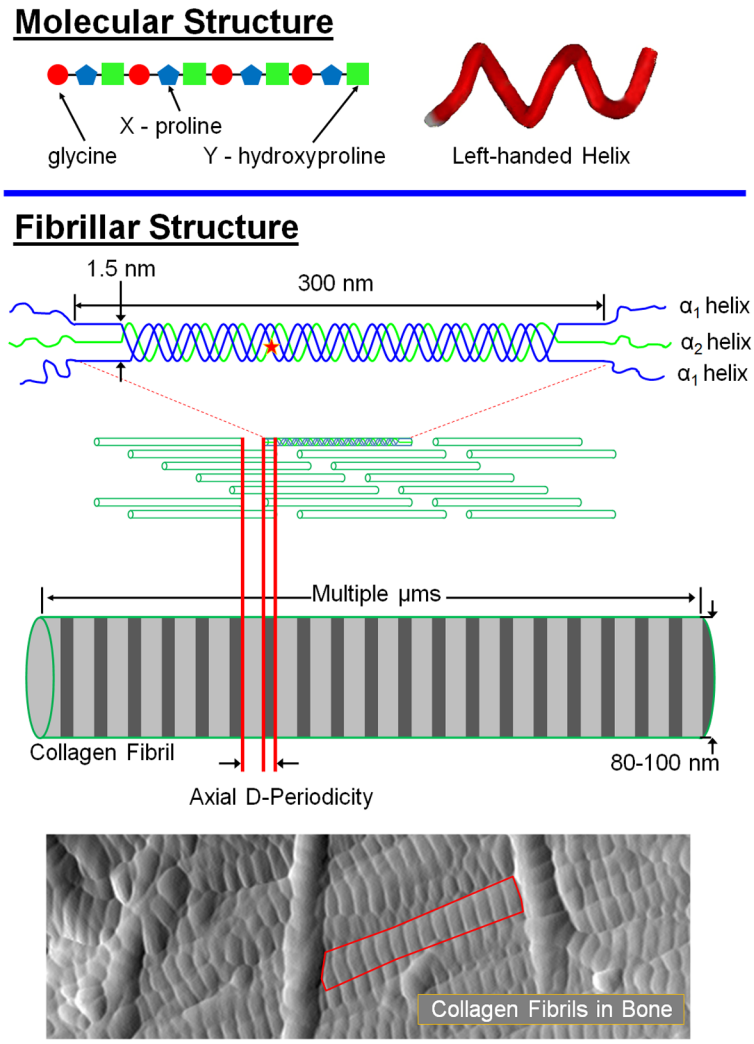

Figure 1. Type I Collagen Fibrillar Organization

Collagen is initially synthesized as a polypeptide chain of amino acids with an uninterrupted region of repeating Gly-X-Y triplets (X and Y are often proline and hydroxyproline, respectively). The significance of glycine being present as every third amino acid is that its small side chain (a single hydrogen atom) can be accommodated within the central axis of the left-handed α helix. Three of these helical chains then form a right-handed triple helix. Once secreted from the cell, non-helical propeptide ends are enzymatically cleaved leaving a 300 nm long, 1.5 nm wide tropocollagen molecule. Tropcollagen molecules self-assemble in a staggered, parallel manner to form a 3D fibril. Because of the space between the ends of the tropocollagen molecules and the offset from row to row, regions of gaps and overlaps exist within the fibril and produce an oscillating surface topography with a characteristic axial repeat pattern called the D-periodicity. In the Brtl/+ disease model, a cysteine residue substitutes for a glycine at the 349 amino acid position in an α1 helix (about 1/3 of the distance in from the left end of the helical portion of the molecules shown above, indicated by the star).

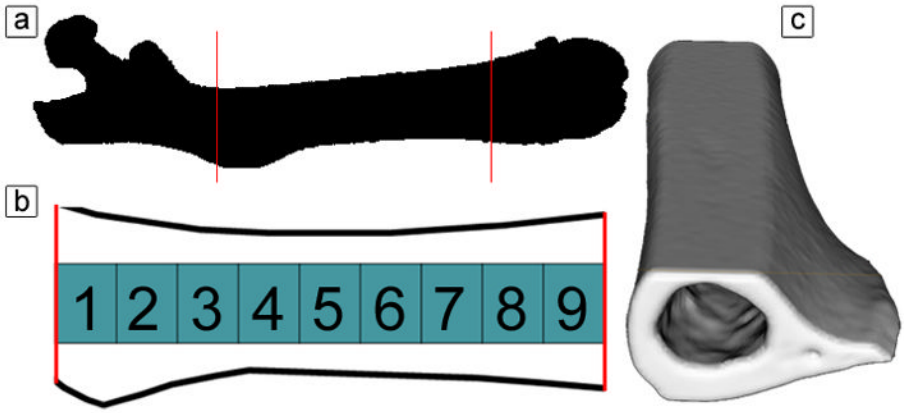

Figure 2. Schematic Representation of the Processed Mouse Femur

Panel a shows a 3D image of a mouse femur, with the anterior surface of the femur facing the reader (proximal end left, distal end right). Along the length of the femur, 9 locations were analyzed to investigate the collagen fibril ultrastructure (panel b). The femur was polished to create a flat intracortical region to image (panel c).

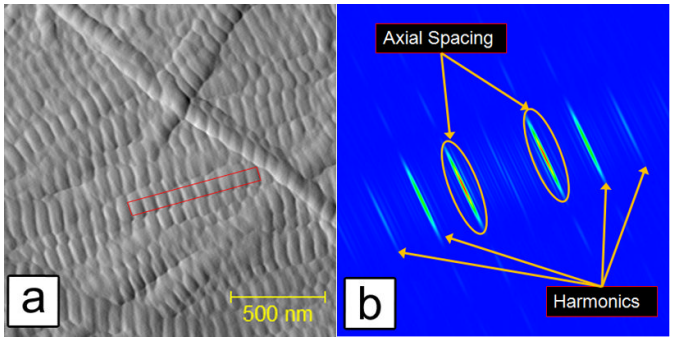

Figure 3. Schematic Representation of Two Dimensional Fast Fourier Transform Measurements

Panel a shows a representative 3.5 μm × 3.5 μm amplitude image that was used to measure the collagen fibril D-periodicity. The box represents a fibril that was chosen for measurement. Panel b shows the corresponding 2D FFT from this fibril. As indicated, the 2D power spectrum contains information about the harmonic characteristics of the fibril. The circled peaks are the first harmonic of the spectrum. The maximum value in this peak corresponds to the D-Periodic repeat distance of the fibril.

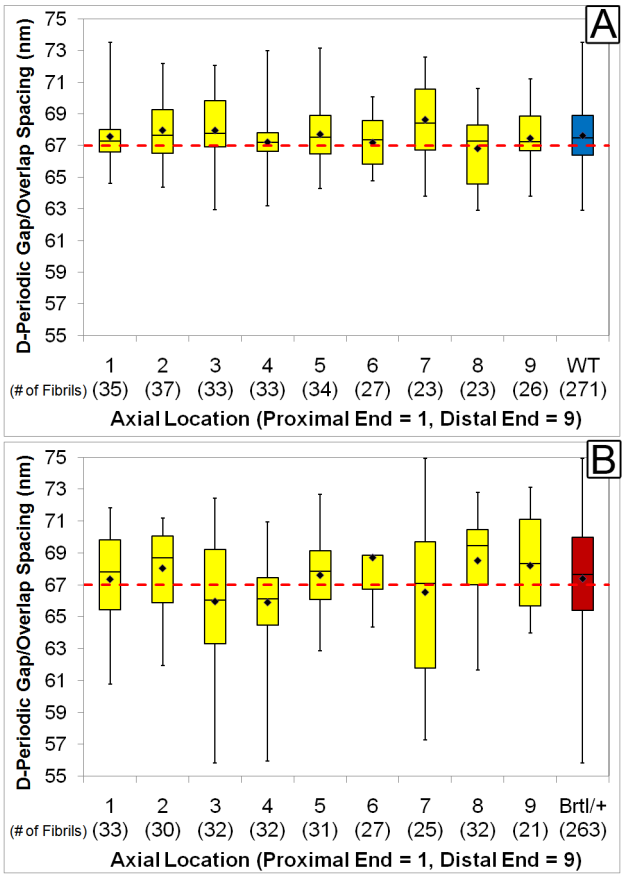

Figure 4. D-Periodic Spacings from Murine Femora as a Function of Axial Location

This figure shows the boxplot representation of the D-periodic spacing from WT (A) and Brtl/+ (B) bones as a function of axial location. The dashed horizontal line indicates the expected 67 nm repeat distance. For each sample, the box is the interquartile region (middle 50% of the data), the horizontal line inside of the box is the median, and the diamond is the mean. The whiskers on the box are the minimum and maximum observation for that location. Qualitatively, there is greater variability between axial locations in the Brtl/+ bones (B) in comparison to the WT (A) bones.

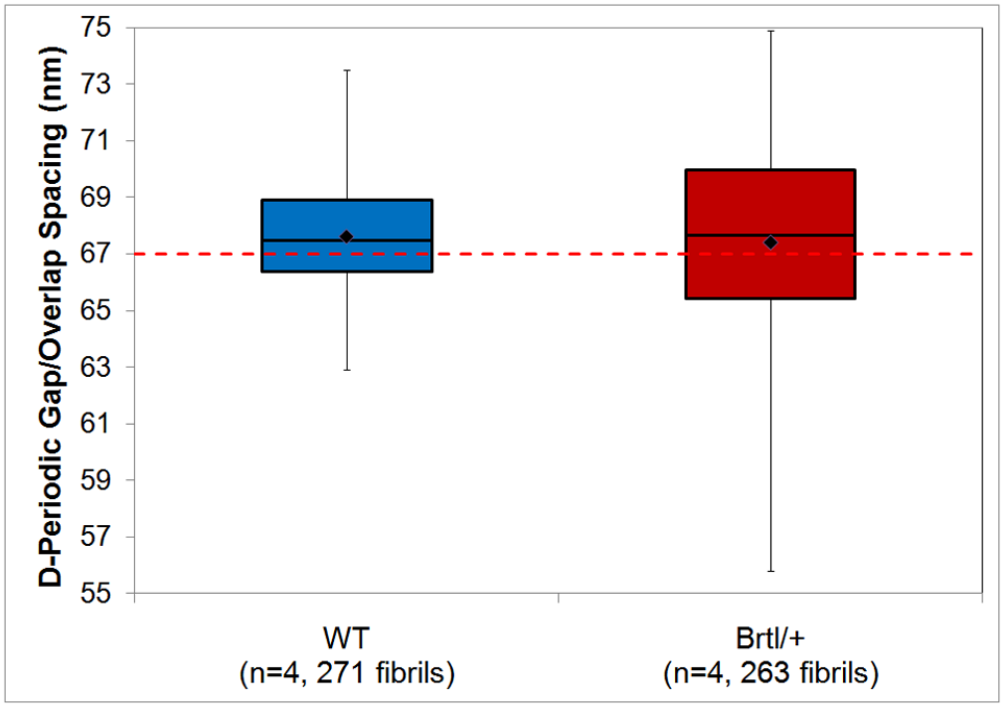

Figure 5. D-Periodic Spacings from Murine Femora

Boxplot representation of the D-periodic spacing from the 4 bones in each genotype. The dashed horizontal line indicates the theoretical 67 nm repeat distance. When the mean values from the 4 samples in each group were compared by One Way ANOVA, WT and Brtl/+ mice ($p=0.392$) did not differ significantly.

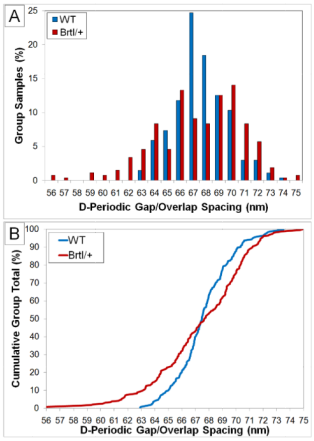

Figure 6. Histogram and Cumulative Density Function of D-Periodic Spacings from Murine Bone

Panel A shows the histogram representation of the D-Periodic spacing from WT and Brtl/+ bones (1 nm bin size). Panel B displays the Cumulative Density Function (CDF) calculated from each group. The CDF shows the fraction of a given sample that is contained up to a particular value. A Kolmogorov-Smirnov test performed on the data distributions indicates that there is a significant differences in the population distributions between WT and Brtl/+mice ($p=0.001$).